An Integrated Control and Readout Circuit for Implantable Multi-Target Electrochemical Biosensing

Sara S. Ghoreishizadeh, Camilla Baj-Rossi, Andrea Cavallini, Sandro Carrara, *Member, IEEE*, and Giovanni De Micheli, *Fellow, IEEE*

***Abstract*—We describe an integrated biosensor capable of sensing multiple molecular targets using both *cyclic voltammetry* (CV) and *chronoamperometry* (CA). In particular, we present our custom IC to realize voltage control and current readout of the biosensors. A mixed-signal circuit block generates sub-Hertz triangular waveform for the biosensors by means of a direct-digital-synthesizer to control CV. A current to pulse-width converter is realized to output the data for CA measurement. The IC is fabricated in 0.18 μm technology. It consumes 220 μW from 1.8 V supply voltage, making it suitable for remotely-powered applications. Electrical measurements show excellent linearity in sub-μA current range. Electrochemical measurements including CA measurements of glucose and lactate and CV measurements of the anti-cancer drug Etoposide have been acquired with the fabricated IC and compared with a commercial equipment. The results obtained with the fabricated IC are in good agreement with those of the commercial equipment for both CV and CA measurements.**

***Index Terms*—Chronoamperometry, cyclic voltammetry, drug detection, glucose sensor, interface electronics, lactate sensor, low frequency waveform.**

I. Introduction

SINCE clinical analysis in clinical laboratories are time-consuming and expensive processes, research is focused on the development of methods to perform rapid measurements of analytes in non-hospital settings, e.g., by patients at home [1]. Electrochemical sensors are ideally suited for these applications by providing rapid, accurate and quantitative detection of analytes with an inexpensive and simple to use setup [2]. The real-time monitoring of metabolites in the blood enables to understand the patient's health condition, whereas the real-time drug monitoring enables the individual adjustment of the drug dosage in order to increase the accuracy and efficacy of the treatment and to reduce dangerous adverse drug reactions, especially for patients with critical or chronic conditions [1], [3]. Endogenous molecules (e.g., glucose, lactate, ATP) and exogenous molecules (e.g., drugs) are among the most important biomolecules to be monitored.

Fully-implantable remotely powered devices are emerging as a valid alternative for continuous monitoring. They eliminate the need for blood sampling and decrease the test costs. The construction of a fully implantable and wireless biosensor requires the integration of three main building blocks: *(i)* a sensor array to detect and measure the target compounds, *(ii)* an interface electronics to control and readout the biosensor, and *(iii)* a power management unit. The implantable device has to be small to be minimally invasive, and low power to be remotely powered. Moreover, it should be able to detect a specific group of key metabolites and drugs within a single platform, to accurately monitor the health condition of the patient and to enable personalized therapy.

The biosensor consists of an array of transducers in a three-electrode configuration to enable multi-target detection. The electrodes are called *working electrode* (WE), *reference electrode* (RE), and *counter electrode* (CE). The WE is where the electrochemical reaction happens, the RE is to control the voltage of the solution while no current flow is allowed on this electrode, and the CE is to close the loop for the sensor current. We presented the design and development of a microfabricated sensor array for multiple-target detection in our previous work [4]. The platform consists of five independent WEs with a common RE and CE in order to allow miniaturization of the platform. Electrodes can be selectively functionalized with carbon-nanotubes and enzymes for the specific detection of target metabolites through *chronoamperometry* (CA) and *cyclic voltammetry* (CV). These are two commonly used electrochemical detection techniques for both endogenous and exogenous molecules [5]. CA and CV measure a current out of a terminal (WE or CE) when a fixed or variable voltage is applied to the other two electrodes, respectively.

Low power CA readout electronics—for glucose or neurotransmitters concentration measurement—in implantable or wearable platforms have been presented in [6]–[9]. In [10]–[14] ICs for CV readout are presented with a control part that is implemented using external waveform generators. In [15] an IC for CA and CV control and readout is presented in 0.5 μm technology. However its power consumption is 20 mW from 5 V supply voltage which makes it difficult to be remotely powered.

In this work a sub-mW fully integrated implementation of CA readout, CV control, and CV readout has been presented.

Manuscript received October 14, 2013; revised January 21, 2014; accepted March 24, 2014. Date of publication June 16, 2014; date of current version January 15, 2015. The research was supported by the Project i-IronIC that is financed with a grant from the Swiss Nano-Tera.ch initiative and evaluated by the Swiss National Science Foundation, and from the SNF Sinergia Project, code CRSII2 127547/1. This paper was recommended by Associate Editor A. Mason.

The authors are with the Integrated System Laboratory, École Polytechnique Fédérale de Lausanne (EPFL), CH-1015 Lausanne, Switzerland (e-mail: seyedehsara.ghoreishizadeh@epfl.ch; camilla.baj-rossi@epfl.ch; andrea.cavallini@epfl.ch; sandro.carrara@epfl.ch; giovanni.demicheli@epfl.ch).

Color versions of one or more of the figures in this paper are available online at http://ieeexplore.ieee.org.

Digital Object Identifier 10.1109/TBCAS.2014.2315157

We describe a low power IC to support both CA and CV for a biosensor array with five sensing sites. A mixed-mode circuit block generates sub-Hertz triangular waveform for the transducer by means of a *direct digital synthesizer* (DDS) to control CV. The CV readout circuit applies the triangular waveform to the WE of interest and reads the bidirectional sensor current at the same WE. A current to pulse-width converter is realized to output the data for CA measurement directly in digital form. To save energy while doing CA measurement, the CV readout circuit can be switched off, and vice versa. The circuit has been implemented in a 0.18 μm technology and successfully tested. A microfabricated sensing platform is used to test the fabricated IC for electrochemical measurements. CA and CV measurements acquired with the fabricated IC are compared with the commercial equipment in terms of sensitivity, linearity, and limit of detection.

In the following section different parts of the interface IC are described. In Section III the measurements with the RC model of the biosensor are presented. Section IV shows the electrochemical measurements performed with the fabricated IC and the comparison with the commercial equipment. The summary and conclusion are in Section V.

II. Circuit Architecture

The interface electronics is divided into four main parts: *(i)* sub-Hertz triangular waveform generator, *(ii)* CV readout, *(iii)* CA readout, *(iv)* potentiostat. The CA readout is designed for unidirectional current measurement, while the CV readout is able to readout bidirectional currents which is necessary in CV mode. Two sensing sites in the sensor array are dedicated to CV readout to measure two anti-cancer drugs (e.g., Etoposide and Mitoxantrone). The other three sensing sites are dedicated to CA readout to measure three endogenous molecules (e.g., Glucose, Lactate and ATP). A multiplexer is used to select the sensor and the readout type.

Fig. 1 shows different parts of the integrated circuit. The circuit is fabricated in 0.18 μm technology and uses a 1.8 V supply voltage. The description of each part is presented here.

A. Triangular Waveform Generator

A fully-on-chip DDS is designed to generate sub-Hertz triangular waveform from a 5 kHz clock frequency. The DDS is realized by mixed-mode design methods. It consists of a 14-bit digital up/down counter and a 9-bit *digital to analog converter* (DAC) (see section I in Fig. 1). The 9 most significant bits of the counter are converted into analog by the DAC. The DAC is implemented in a resistor ladder scheme. To provide different slopes needed for electrochemical sensor conditioning and measurement, the waveform generator is designed to be configurable. The up/down counter step size which is determined by the *slope control*, sets the slope of the waveform.

B. CV Readout

To control the sensor in CV mode, a fixed voltage of 0.9 V is applied to the RE through the potentiostat while the triangular waveform is applied to the WE of interest. Therefore, the cell voltage $(V_{WE} - V_{RE})$ sweeps both negative and positive voltages. The bidirectional sensor current (I_{WE}) is read through a trans-impedance amplifier as shown in section II of Fig. 1. OP_1 applies the triangular waveform to the WE and the resulted current flows through R_M. OP_1 is a folded cascode with NMOS and PMOS input stage and class-A output stage as shown in Fig. 2. Its gain, -3 dB bandwidth, power consumption and phase margin are 70 dB, 100 Hz, 28 μW, and 75° (for load capacitance of 1 nF), respectively. The load of OP_1 is the electrochemical sensor. Since the RC equivalent model of an electrochemical sensor is known to be time and concentration dependent [5], OP_1 is compensated using the method in [16] to have

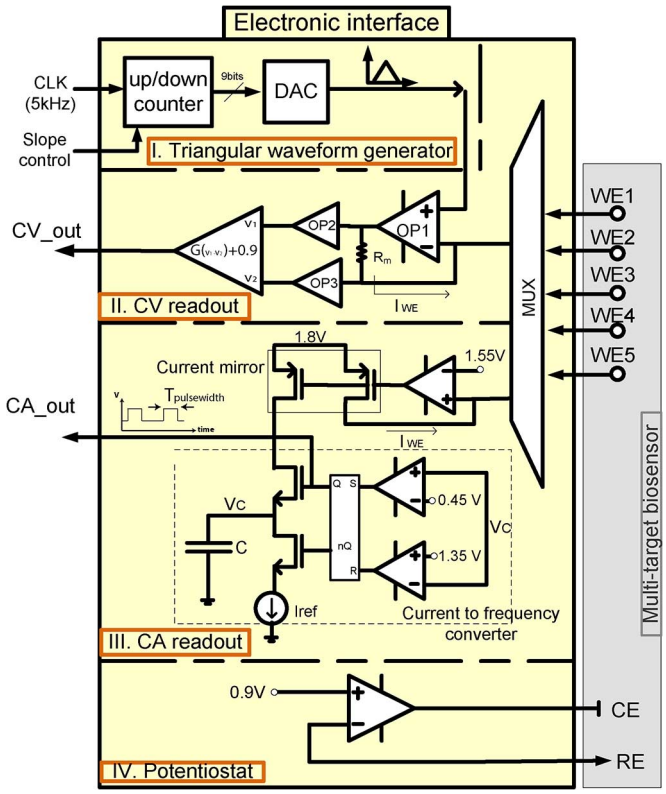

Fig. 1. Schematic view of the sensor driver/readout interface for a multi-target electrochemical biosensor. It consists of 4 main circuits: waveform generator, CA readout, CV readout, and potentiostat.

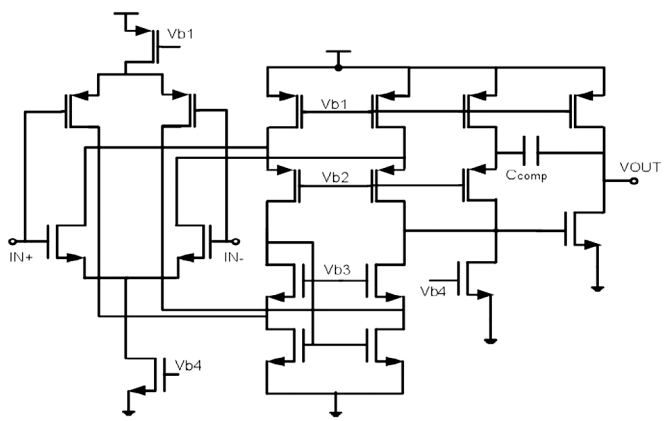

Fig. 2. Schematic view of two-satge opamp with NMOS and PMOS input stages, and a class A output stage, compensated for a wide range of load capacitance. This structure is used for both OP_1 and potentiostat in Fig. 1. All the bias voltages are generated on-chip.

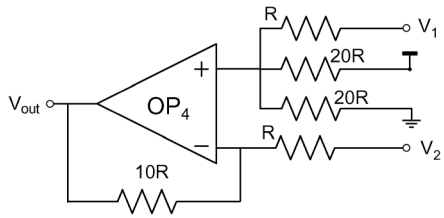

Fig. 3. Schematic view of the last stage of the CV readout circuit. It consists of OP_4 and poly resistors. It amplifies the difference between V1 and V2 by a factor of 10 and shifts the resulted voltage up by $V_{DD}/2$.

a phase margin of more than 45° for any load capacitance more than 100 pF.

The voltage across R_M is buffered through OP_2 and OP_3. Since the common mode voltage across the resistor can be any value form 0.1 V to 1.7 V (due to the sensor current range and R_M), OP_2 and OP_3 are designed to have full swing input and outputs. The last stage in CV readout circuit is a common difference amplifier shown in Fig. 3. It consists of OP_4 which is designed similar to OP_1, and poly resistors with low temperature coefficient. This block amplifies the buffered voltage across the resistor R_M, and adds a DC voltage of $V_{DD}/2$ to it so that its output stays within the supply voltage range. The output voltage of the CV readout is

$$V_{CV_{out}} = G \times R_m \times I_{WE} + V_{shift} \tag{1}$$

where G and V_{shift} are the gain and DC shift voltage by the last stage in CV readout, respectively. G is equal to 10 and V_{shift} is 0.9 V.

C. CA Readout

In CA, a fixed voltage is applied to the sensor and the resulted unidirectional current is measured. The circuit for CA measurement is shown in section III of Fig. 1. It consists of two main blocks: *(i)* a circuit to apply a fixed voltage to the WE and current mirrors to generate a copy of the sensor current; *(ii)* a current to pulse-width converter similar to [6]. The pulse width is inversely proportional to the sensor current and can be calculated by

$$T_{pulse-width} = \frac{C(V_1 - V_2)}{I_{WE}}. \tag{2}$$

The CA readout circuit converts the sensor current into a digital waveform which can easily be transmitted outside the implantable (e.g., by backscattering) without any need to an analog to digital converter.

D. Potentiostat

The potentiostat applies a fixed voltage to the RE using a negative feedback around RE and CE and provides current to the CE (see section IV in Fig. 1). Since RE and CE are shared among all five sensors, the potentiostat is used for both kinds of readout. The implemented potentiostat is a two stage folded cascode amplifier with class-A second stage. It is compensated using the method in [16] and its phase margin remains greater than 45° for any load capacitance higher than 400 pF. The gain, −3 dB bandwidth, and power consumption of the potentiostat are 65 dB, 175 Hz, 37 μW, respectively. The layout of the fabricated IC in 0.18 μm technology is shown in Fig. 4. The power consumption of different blocks are reported in Table I.

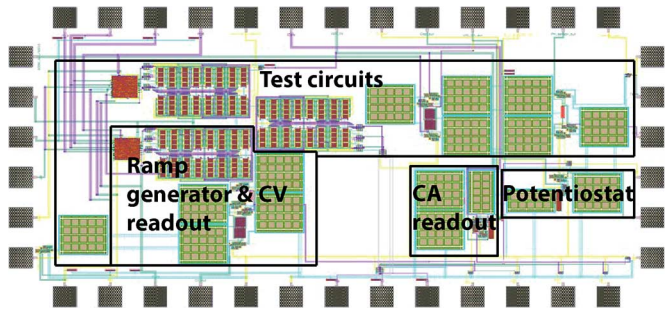

Fig. 4. Layout of the IC in 0.18 μm technology.

TABLE I
POWER CONSUMPTION OF DIFFERENT BLOCKS OF THE IC FORM SIMULATIONS

Block name	*Power consumption (μW)*
Waveform generator	3.5
CV readout	117
CA readout	63
Potentiostat	36.5
Total	220

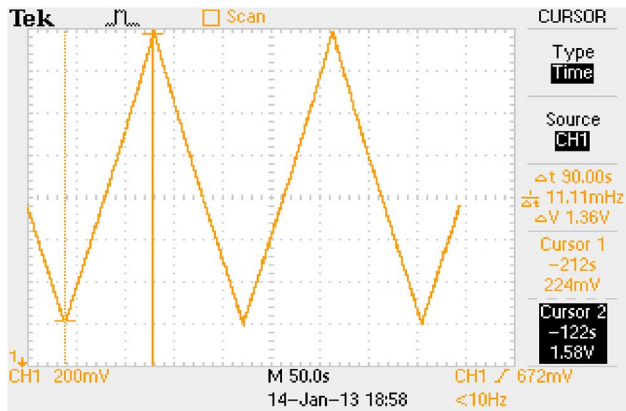

Fig. 5. The measured sub-Hertz triangular waveform to control the sensor in CV by the on-chip waveform generator. Its min, max and frequency are 0.2 V, 1.6 V, and 5.5 mHz, respectively.

III. ELECTRICAL MEASUREMENT

The measured sub-Hertz triangular waveform generated by the on-chip waveform generator is shown in Fig. 5. The slope of the triangular waveform can be adjusted to 64 different values from 15 mV/s (Fig. 5) to 130 V/s to address different needs in sensor measurement and conditioning. The measured maximum, minimum and the step size of the generated triangular waveform are 1.6 V, 0.2 V and 3.2 mV, respectively. The measured characteristics of the triangular waveform are summarized in Table II. CA readout circuit is tested by applying a current between 40 nA and 1 μA to the WE connected to the circuit and a reference current (I_{ref} in Fig. 1) of 1.93 μA. The resulted pulse-width is measured, using a Tektronix TDS2014B

TABLE II
MEASURED SPECIFICATIONS OF THE TRIANGULAR WAVEFORM

Parameter	*Value*
min-max	0.2 V-1.6 V
step size	3.2 mV
slope	15 mV/s to 130 V/s
Supply voltage	1.8 V
input Clock frequency	5 kHz

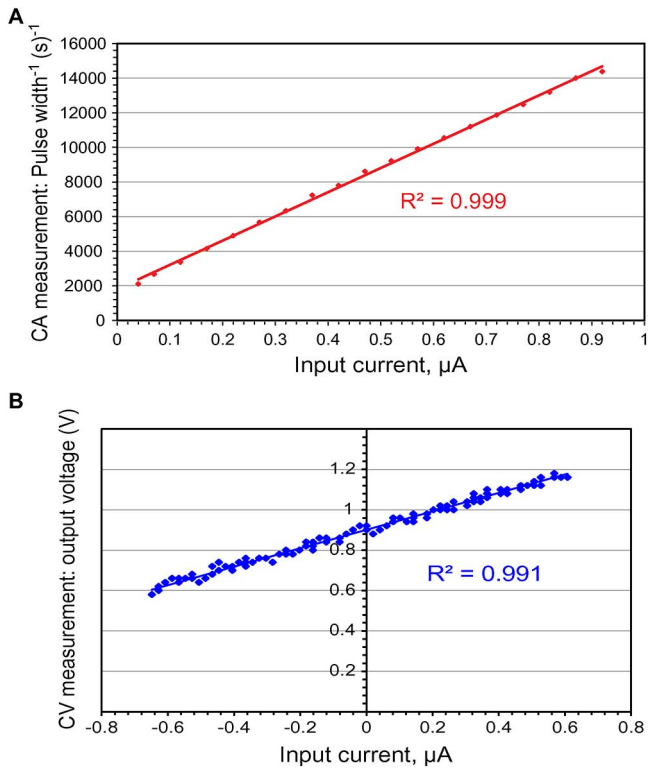

Fig. 6. Measured characteristics of the circuits for (a) CA and (b) CV readout. The input current is converted to voltage in CV and to pulse width in CA. The internally generated sub-Hertz triangular waveform is applied to control CV measurement.

digital oscilloscope, for different input currents. The inverse of the pulse-width versus the input current is plotted in Fig. 6(a). The measurements show excellent linearity in sub-μA current range. In order to test the CV readout, the internally generated triangular waveform with the slope of 130 V/s is applied to the positive terminal of OP_1, while the negative terminal of OP_1 (i.e., WE) is connected to a resistor R_{test}. The other terminal of R_{test} is connected to CE terminal of the potentiostat, while the potentiostat is connected as a unity gain buffer (i.e., RE and CE are short connected) and a voltage of 0.9 V is applied to its positive terminal. Therefore the input current of the CV readout circuit can be calculated by

$$I_{res} = \frac{V_{ramp} - 0.9}{R_{test}}. \tag{3}$$

The measured voltage at the output of CV readout circuit is plotted versus the input current in Fig. 6(b) for a R_{test} of 987 kΩ.

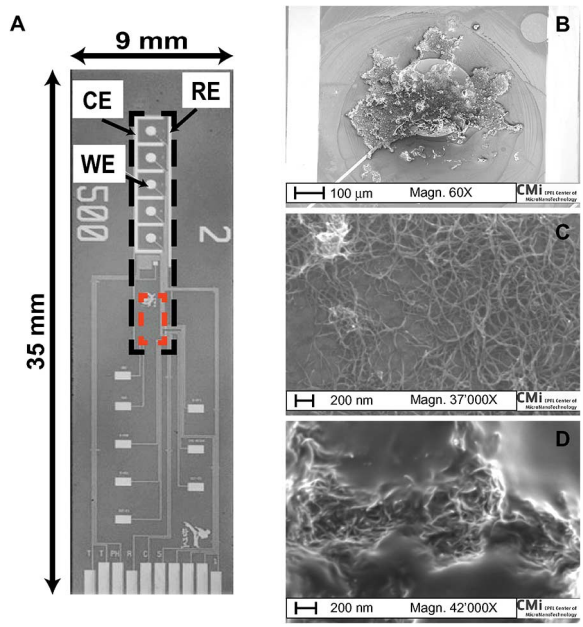

Fig. 7. Biosensor. (a) Micro-fabricated sensor that hosts five WEs, a common counter and reference electrode. The black dashed line defines the section of the platform that is diced to be integrated in the implantable sensor reported in Fig. 11. The red dashed line define the space for bonding the IC. (b) SEM image of MWCNTs drop-cast on a WE. (c) At higher magnification. (d) SEM image of MWCNTs and GOx drop-cast on a WE.

IV. ELECTROCHEMICAL MEASUREMENT

The fabricated circuit is designed to work in combination with the sensor array shown in Fig. 7. The CA and CV measurements acquired with the sensor array and the control/readout IC are presented in this section.

A. Materials and Methods

1) Chemicals: Multi-walled carbon nanotubes (MWCNTs, $\sim$10 nm diameter and $\sim$1–2 μm length) with 5%—COOH groups content, were purchased as a powder (90% purity) from DropSens. A 1 mg/ml solution of MWCNTs, prepared in chloroform, was sonicated for 30 min to obtain a homogeneous suspension [17]. Milli-Q water (18 MΩ/cm) was used to prepare all aqueous solutions. All experiments were carried out in a 100 mM *phosphate buffered saline* (PBS) solution (pH 7.4) as supporting electrolyte.

Glucose oxidase (GOx) from *Aspergillus Niger* and *lactate oxidase* (LOx) from *Pediococcus species* were purchased from Roche in lyophilizate powder and dissolved in a 100 mM PBS (pH 5.86). $D-(+)$-glucose and lithium L-lactate were purchased from Sigma-Aldrich in powder and dissolved in in Milli-Q water. Etoposide was purchased as a powder from Sigma-Aldrich. Due to its low solubility in water, Etoposide solutions at different concentration were prepared by dissolving it in Dimethyl sulfoxide (from Sigma Aldrich) before storage at room temperature.

2) Sensor Array Microfabrication: Microfabrication was realized at the EPFL Centre of Micronano Technology (CMI). Silicon wafers with 500 nm of native oxide were chosen as substrate. Chip metalization was realized by evaporation of 10 nm of Ti, followed by 100 nm of Pt. Metal passivation was made

by atomic layer deposition of Al_2O_3 20 nm, followed by dry etching with Argon Ion Milling.

The sensor array has five WEs (with a diameter of 500 μm), a common RE and a common CE, all made in Pt. Fig. 7(a) shows a microphotograph of the micro-fabricated platform where the structure of the electrodes are visible. The black dashed line in this figure defines a section of the platform which is 2.2 $\times$ 15 mm and is diced to be integrated in the implantable sensor. The red dashed line defines the space for the bonding of the fabricated IC. Details on the microfabrication of the platform can be found in [4].

3) Electrode Functionalization: For the glucose and lactate detection, WEs were nanostructured with 0.2 μg of MWCNTs and a drop of 15 mg/ml GOx and 33 mg/ml LOx respectively. They were stored overnight at 4°C. All the samples were freshly prepared and used the same day. When not in use, electrodes were stored at 4°C. For the measurements in CV, the electrodes were used without modifications. In Fig. 7(b) a *Scanning Electron Microscope* (SEM) image of a WE after the drop-cast of MWCNTs is shown. Fig. 7(c) shows a larger magnification in which the three-dimensional structure of carbon nanotubes on the electrode surface is visible. Fig. 7(d) shows the difference when the protein (GOx) is cast on the WE with MWCNT. The SEM images were acquired using a SEM LEO 1550 manual microscope.

4) Measurements: Electrochemical measurements were performed using the IC and repeated with an Autolab (Metrohm) electrochemical workstation, on the same day, for comparison. The very same sensing sites of the sensor array were used for the measurements with the IC and Autolab. Electrodes were tested for glucose and lactate sensitivity with CA at +650 mV. The sensors were first dipped in 8 ml PBS (100 mM, pH 7.4) under stirring conditions, and conditioned for one hour at +650 mV. Then they are tested with successive injections of glucose 500 μM or lactate 50 μM.

CV was used to identify the oxidation/reduction peaks of Etoposide. CV were performed at room temperature under aerobic conditions by applying a triangular waveform with a minimum of -300 mV, maximum of +900 mV versus the RE and a slope of 68 mV/s. The sensor was dipped into 8 ml of 100 mM PBS (pH 7.4) and Etoposide was injected at concentrations of 200 μM and 400 μM after an initial 5 minute conditioning.

Sensitivity and *limit of detection* (LOD) are the key parameters to evaluate the sensing performances. Sensitivity per unit area was computed from the slope of the calibration line obtained by plotting the current steps versus the metabolite (e.g., glucose or lactate) concentration. The LOD was computed according to the expression

$$LOD = k\frac{\delta i}{S} \tag{4}$$

where delta i is the standard deviation of the blank measurements, S is the sensitivity, and k is a parameter accounting for the confidence level ($k = 1$, 2, or 3 corresponds to 68.2%, 95.4%, or 99.6% of statistical confidence), according to [18]–[20].

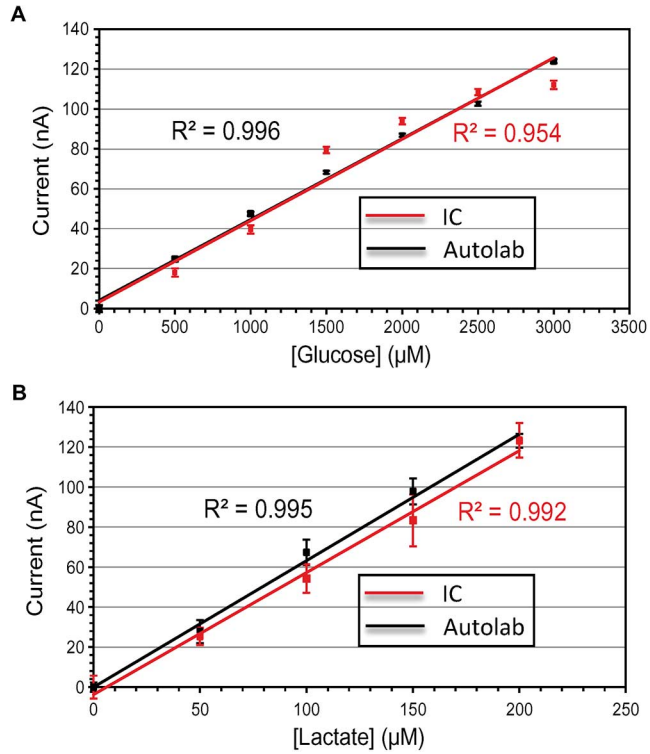

Fig. 8. Comparison of the calibration curves for (a) glucose and (b) lactate obtained with the IC (in red) and Autolab (in black). The error bars for the case of IC are due to the variations of the measured average frequency. In the case of Autolab, the error bars are standard deviation of the measured current.

TABLE III
COMPARISON IN SENSITIVITY AND LOD BETWEEN THE IC AND THE AUTOLAB FOR GLUCOSE AND LACTATE DETECTION

	Sensitivity ($\frac{mA}{mM \times cm^2}$)		*LOD* (μM)	
Metabolite	IC	Autolab	IC	Autolab
Glucose	27.2±5.2	27.3±0.5	87.9±22	17.5±1.4
Lactate	286±42.9	322±48.3	21.4±5.1	4.1±0.9

B. Results

1) CA: The CA measurements at +650 mV for glucose and lactate obtained with the IC are reported in Fig. 8(a) and (b), respectively. Measurements acquired with the Autolab are also shown for comparison. In these graphs, the vertical axis is the measured sensor current which is calculated using the calibration line in Fig. 6(a). Table III reports the sensitivity and LOD for glucose and lactate obtained with the IC and the Autolab. The differences in biosensor sensitivities when measured with the IC and Autolab are 0.4% for glucose and 11% for lactate. This can be fully attributed to the nature of the biosensors as it is widely demonstrated that the sensitivity of the biosensor changes considerably when measured at different times [21]–[24]. In the case of glucose, the Food and Drug Administration (FDA) regulates the blood glucose meters using guidelines issued by the International Organization for Standardization (ISO) 15197:2003, *Requirements for blood glucose monitoring systems for self testing in managing diabetes mellitus*. The ISO standard requires that 95% of results

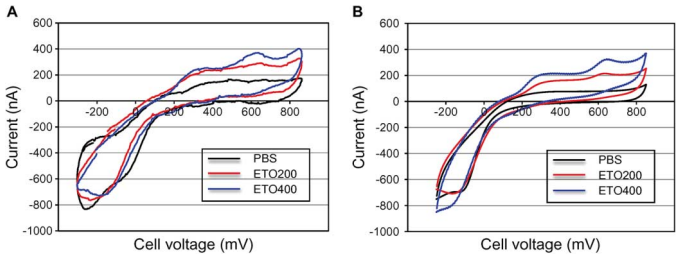

Fig. 9. CV with the bare electrode in PBS, Etoposide (ETO) 200 μM and ETO 400 μM obtained with (a) the IC and (b) the Autolab.The slope of the applied voltage is 68 mV/s.

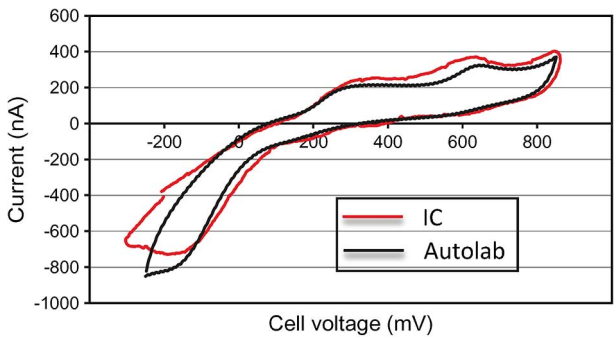

Fig. 10. Comparison between the IC and the Autolab for the CV obtained in presence of Etoposide 400 μM.

within range or slightly elevated be within $\pm$20% of the true value. Assuming that the current measured with the Autolab is the *true current*, the presented biosensing platform fulfils this requirement: according to Fig. 8(a), the measured glucose sensor current with the IC in different glucose concentrations is within $\pm$20% of the current measured with the Autolab.

The higher LOD in the measurements with the IC is due to the limited accuracy of and higher noise in the measurement setup with the IC.

With the fabricated IC we were able to detect glucose and lactate in low concentration ranges (500–3000 μM for glucose and 50–200 μM for lactate), that are relevant in many clinical applications [25], [26].

2) CV: The anti-cancer drug Etoposide was chosen for CV measurement because it is an electro-active compound that gives two well-defined oxidation peaks at around +600 mV and +300 mV in CV [27].

Fig. 9 compares the CVs for Etoposide at the concentration of 0 μM, 200 μM and 400 μM, obtained with the fabricated IC [Fig. 9(a)]and Autolab [Fig. 9(b)]. In both cases two peaks at +300 mV and +600 mV are increasing with Etoposide concentration. For a better comparison Fig. 10 shows the CV at Etoposide 400 μM acquired with the IC (in red) and with the Autolab (in black). A low pass filter is applied to the data from the measurements with IC to reduce the noise. To keep the voltage of CE within the supply voltage range (0 to 1.8 V) we used an extra CE with an effective size of $\sim$ 0.126 cm^2. A bigger CE electrode decreases the resistance between CE and RE, and consequently the voltage drop between CE and RE. The area of the CE will be increased for CV measurements in the next sensor array fabrication.

TABLE IV
COMPARISON BETWEEN THE IC AND THE AUTOLAB FOR THE PEAK ATTRIBUTED TO THE OXIDATION OF ETOPOSIDE

	Peak current location (mV)		*Peak Current (nA)*	
[Etoposide]	IC	Autolab	IC	Autolab
200 μM	613$\pm$18.4	617$\pm$18.5	39.6$\pm$6.7	45.4$\pm$3.2
400 μM	610$\pm$18.3	631$\pm$18.9	79.3$\pm$3.2	71.2$\pm$4.3

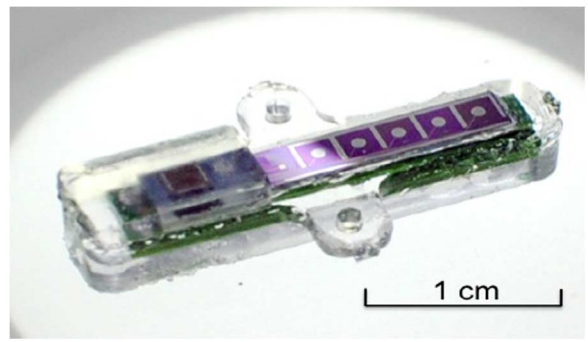

Fig. 11. Photograph of the fabricated IC and the multi-target sensor in a biocompatible package.

Table IV reports the voltage and the current value of the Etoposide oxidation peak at +600 mV calculated from the CV measurements shown in Fig. 9. The measured peak position with the IC is less than 3.5% different from the same measurement with Autolab, that compares quite well with measurements errors of about 3% registered with both the IC and the Autolab.

V. SUMMARY AND FUTURE WORKS

An integrated circuit in 0.18 μm has been designed to control and readout an array of biosensors. The sensing sites in the sensor array can be readout in both CA and CV. A sub-Hertz triangular waveform is generated by an on-chip DDS to control the CV measurement. A current to frequency converter is designed for CA readout. Measurements show excellent linearity in sub-μA range. Glucose and lactate CA measurements with the IC have a LOD of 87.9 and 21.4 μM and sensitivity of 27.2 and 285.7 μA/(mM $\times$ cm^2), respectively. Etoposide CV measurement is achieved by applying the on-chip triangular waveform with the slope of 68 mV/s to the sensor. The oxidation current peak position and height agrees well with the measurements performed with the commercial equipment. The IC consumes 220 μW from 1.8 V supply voltage which makes it suitable for remotely powered implantable applications [28].

We demonstrated that the fabricated IC efficiently works for the control and readout of the sensor array in both CA and CV with the present work. Next step will be the integration of an ADC to the CV readout to enable the communication and to realize a fully-integrated and implantable biosensor platform for *in-vivo* tests. The first prototype of such integration in a bio-compatible package is presented in Fig. 11. In addition to the present IC and the sensor array, the prototype includes a receiving coil and a power management IC for the remote powering of the device [29], [30]. Corrosion of electronic components and leaking of potentially hazardous substances in the body is prevented with a conformal coating of Parylene C, while

an outer package of medical grade silicone was employed to create a soft shell suitable for implantation. The size of the packaged device is $3 \times 3 \times 19$ mm (without the wings, each wing is $1 \times 2 \times 3$ mm). Details about the sensors, soft packaging and the bio-compatibility of the first prototype can be found in [31], [32].

ACKNOWLEDGMENT

The authors would like to thank I. Taurino for the SEM images acquisition, and C. Boero for helping to proofread this paper.

REFERENCES

[1] C. Hiemke, "Clinical utility of drug measurement and pharmacokinetics—Therapeutic drug monitoring in psychiatry," *Eur. J. Clin. Pharmacol.*, vol. 64, no. 2, pp. 159–166, 2008.

[2] P. D'Orazio, "Biosensors in clinical chemistry- 2011 update," *Clinica Chimica Acta*, vol. 412, no. 19, pp. 1749–1761, 2011.

[3] A. S. Gross, "Best practice in therapeutic drug monitoring," *Brit. J. Clin. Pharmacol.*, vol. 46, no. 2, pp. 95–99, 2002.

[4] A. Cavallini, C. Baj-Rossi, S. S. Ghoreishizadeh, G. De Micheli, and S. Carrara, "Design, fabrication, test of a sensor array for perspective biosensing in chronic pathologies," in *Proc. IEEE Biomedical Circuits and Systems Conf.*, 2012, pp. 124–127.

[5] A. J. Bard and L. R. Faulkner, *Electrochemical Methods: Fundamentals and Applications*. New York, NY, USA: Wiley, 1980.

[6] M. M. Ahmadi and G. A. Jullien, "Current-mirror-based potentiostats for three-electrode amperometric electrochemical sensors," *IEEE Trans. Circuits Syst. I, Reg. Papers*, vol. 56, no. 7, pp. 1339–1348, 2009.

[7] M. Haider, S. Islam, S. Mostafa, M. Zhang, and T. Oh, "Low-power low- voltage current readout circuit for inductively powered implant system," *IEEE Trans. Biomed. Circuits Syst.*, vol. 4, no. 4, pp. 205–213, Aug. 2010.

[8] L. Yu-Te, Y. Huanfen, A. Lingley, B. Parviz, and B. P. Otis, "A 3-μW CMOS glucose sensor for wireless contact-lens tear glucose monitoring," *IEEE J. Solid-State Circuits*, vol. 47, no. 1, pp. 335–344, 2012.

[9] M. Stanacevic, K. Murari, A. Rege, G. Cauwenberghs, and N. V. Thakor, "VLSI potentiostat array with oversampling gain modulation for wide-range neurotransmitter sensing," *IEEE Trans. Biomed. Circuits Syst.*, vol. 1, no. 1, pp. 63–72, 2007.

[10] A. Hassibi and T. H. Lee, "A programmable 0.18- μm CMOS electrochemical sensor microarray for biomolecular detection," *IEEE Sensors J.*, vol. 6, no. 6, pp. 1380–1388, 2006.

[11] R. J. Reay, S. P. Kounaves, and G. T. A. Kovacs, "An integrated CMOS potentiostat for miniaturized electroanalytical instrumentation," in *Proc. IEEE Int. Solid-State Circuits Conf.*, 1994, pp. 162–163.

[12] M. Nazari and R. Genov, "A fully differential CMOS potentiostat," in *Proc. IEEE Int. Symp. Circuits and Systems*, 2009, pp. 2177–2180.

[13] H. M. jafari and R. Genov, "Chopper-stabilized bidirectional current acquisition circuits for electrochemical biomolecular detection," *IEEE Trans. Circuits Syst. I, Reg. Papers*, vol. 60, no. 5, pp. 1149–1157, 2013.

[14] P. Levine, P. Gong, R. Levicky, and K. L. Shepard, "Active CMOS sensor array for electrochemical biomolecular detection," *IEEE J. Solid-State Circuits*, vol. 43, no. 8, pp. 1859–1871, 2008.

[15] L. Li, L. Xiaowen, W. A. Qureshi, and A. J. Mason, "CMOS amperometric instrumentation and packaging for biosensor array applications," *IEEE Trans. Biomed. Circuits Syst.*, vol. 5, no. 5, pp. 439–448, Oct. 2011.

[16] B. K. Ahuja, "An improved frequency compensation technique for CMOS operational amplifiers," *IEEE J. Solid-State Circuits*, vol. 18, no. 6, pp. 629–633, 1983.

[17] C. Baj-Rossi, G. De Micheli, and S. Carrara, "Electrochemical detection of anti-breast-cancer agents in human serum by cytochrome P450-coated carbon nanotubes," *Sensors*, vol. 5, no. 5, pp. 6520–6537, 2012.

[18] S. Carrara, A. Cavallini, V. Erokhin, and G. De Micheli, "Multi-panel drugs detection in human serum for personalized therapy," *Biosens. Bioelectron.*, vol. 26, no. 9, pp. 3914–3919, 2011.

[19] J. Mocak, A. M. Bond, S. Mitchell, and G. Scollary, "A statistical overview of standard (IUPAC and ACS) and new procedures for determining the limits of detection and quantification: Application to voltammetric and stripping techniques," *Pure Appl. Chem.*, vol. 69, no. 2, pp. 297–328, 1997.

[20] J. N. Miller and J. C. Miller, *Statistics and Chemometrics for Analytical Chemistry*, 6th ed. Englewood Cliffs, NJ, USA: Prentice Hall, 2005.

[21] I. Taurino, R. Reiss, M. Richter, M. Fairhead, and L. Thoeny-Meyer *et al.*, "Comparative study of three lactate oxidases from aerococcus viridans for biosensing applications," *Electrochim. Acta*, vol. 93, pp. 72–79, 2013.

[22] A. Biedler, S. Schneider, F. Bach, S. Soltesz, W. Wilhelm, S. Ziegeler, and S. Kreuer, "Methodological aspects of lactate measurement evaluation of the accuracy of photometric and biosensor methods," *Open Anesthesiol. J.*, vol. 1, pp. 1–5, 2007.

[23] D. B. Pyne, T. Boston, D. T. Martin, and A. Logan, "Evaluation of the lactate pro blood lactate analyser," *Eur. J. Appl. Physiol.*, vol. 82, pp. 112–116, 2000.

[24] M. Florescu and C. M. A. Brett, "Development and evaluation of electrochemical glucose enzyme biosensors based on carbon film electrodes," *Talanta*, vol. 65, pp. 306–312, 2005.

[25] V. H. Routh, "Glucose-sensing neurons: Are they physiologically relevant?," *Phys. Behav.*, vol. 76, no. 3, pp. 403–413, 2002.

[26] M. J. Markuszewski, K. Otsuka, S. Terabe, K. Matsuda, and T. Nishioka, "Analysis of carboxylic acid metabolites from the tricarboxylic acid cycle in Bacillus subtilis cell extract by capillary electrophoresis using an indirect photometric detection method," *J. Chromatogr. A*, vol. 1010, no. 1, pp. 113–121, 2003.

[27] J. J. M. Holthuis, W. J. Van Oort, F. M. G. M. Romkens, and J. Renema, "Electrochemistry of podophyllotoxin derivatives: Part I. Oxidation mechanism of Etoposide (VP 16-213).," *J. Electroanal. Chem. Interfacial Electrochem.*, vol. 184, no. 2, pp. 317–329, 1985.

[28] J. Olivo, S. Carrara, and G. De Micheli, "Energy harvesting and remote powering for implantable biosensors," *IEEE Sensors J.*, vol. 11, no. 7, pp. 1573–1586, 2011.

[29] J. Olivo, S. Carrara, and G. De Micheli, "A study of multi-layer spiral inductors for remote powering of implantable sensors," *IEEE Trans. Biomed. Circuits Syst.*, vol. 7, no. 4, pp. 536–547, Aug. 2013.

[30] J. Olivo, S. Ghoreishizadeh, S. Carrara, and G. De Micheli, "Electronic implants: Power delivery and management," in *Proc. Design, Automation and Test in Eur. Conf. and Exhib.*, 2013, pp. 1540–1545.

[31] S. Carrara, A. Cavallini, S. Ghoreishizadeh, J. Olivo, and G. De Micheli, "Developing highly-integrated subcutaneous biochips for remote monitoring of human metabolism," in *Proc. IEEE Sensors Conf.*, 2012.

[32] A. Cavallini, "An implantable biosensor array for personalized therapy applications," Dissertation, Lausanne, Switzerland, 2013.

Sara S. Ghoreishizadeh received the B.Sc degree in electrical engineering and M.Sc. degree in microelectronics circuits from the Sharif University of Technology, Tehran, Iran, in 2007 and 2009, respectively.

Currently, she is a Research Assistant and doctoral candidate in the Integrated Systems Laboratory at École Polytechnique Fédérale de Lausanne, Lausanne, Switzerland. Her research is focused on design and implementation of low power analog/mixed-signal IC to readout, control, and calibrate multi-target electrochemical biosensors. Her research interests include designing dedicated circuits for health care monitoring and personalized therapy within highly-integrated implantable devices.

Camilla Baj-Rossi received the M.Sc. degree in biomedical engineering from Politecnico di Torino, Torino, Italy, in 2010.

She carried out research for her master's thesis with École Polytechnique Fédérale de Lausanne (EPFL), Lausanne, Switzerland. Currently, she is working toward the Ph.D. degree in the Laboratory of Integrated Systems, EPFL. Her research interests include the development of a point-of-care biosensor array based on multiwalled carbon-nanotubes and enzymes to detect drugs and metabolites in biological fluids.

Andrea Cavallini received the M.Sc. degree (with honors) in biomolecular biotechnology from the University of Bologna, Bologna, Italy, and the Ph.D. degree in biosensors and bioengineering from the Swiss Federal Institute of Technology, Lausanne, Switzerland, in 2008 and 2013, respectively.

Currently, he is working at Qloudlab SA, Lausanne, Switzerland, to develop a portable blood diagnostic test for blood analysis with smartphones. He earned the Best Poster Award at the 7th NanoEurope Symposium (2009) and the Bronze Leaf Paper Award at the PRIME Conference (2010).

Sandro Carrara (M'09) received the M.Sc. degree from the University of Genoa, Genoa, Italy, and the Ph.D. degree in biochemistry and biophysics from the University of Padua, Padova, Italy, in 1993 and 1997, respectively.

He is a Lecturer at École Polytechnique Fédérale de Lausanne (EPFL), Lausanne, Switzerland. He is a former Professor of optical and electrical biosensors in the Department of Electrical Engineering and Biophysics (DIBE), University of Genoa, and a former Professor of nanobiotechnology at the University of Bologna, Italy. His scientific interests are on electrical phenomena of nano-biostructured films, and include CMOS design of biochips based on proteins and DNA. He has authored more than 170 scientific publications and 12 patents. He has had several Top 25 Hottest Articles (2004, 2005, 2008, 2009, and twice in 2012) published in highly-ranked international journals.

Dr. Carrara is founder and Editor-in-Chief of the journal *BioNanoScience*, Topical Editor of the IEEE SENSORS JOURNAL, and Associate Editor of the IEEE TRANSACTIONS ON BIOMEDICAL CIRCUITS AND SYSTEMS. He is a member for the IEEE Circuits and Systems Society (CASS) and member of the Board of Governors of the IEEE Sensors Council. He has been appointed as CASS Distinguished Lecturer for 2013–2014. He is the General Chairman of the BioCAS Conference in 2014.

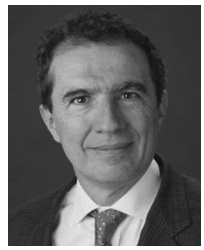

Giovanni De Micheli (F'94) received the nuclear engineer degree from Politecnico di Milano, Italy, in 1979, and the M.S. and Ph.D. degrees in electrical engineering and computer science from the University of California, Berkeley, CA, USA, in 1980 and 1983, respectively.

Currently, he is a Professor and Director of the Institute of Electrical Engineering and of the Integrated Systems Centre at École Polytechnique Fédérale de Lausanne (EPFL), Lausanne, Switzerland. He is Program Leader of the Nano-Tera.ch program. Previously, he was Professor of Electrical Engineering at Stanford University, Stanford, CA, USA. His research interests include several aspects of design technologies for integrated circuits and systems, such as synthesis for emerging technologies, networks on chips and 3D integration. He is also interested in heterogeneous platform design including electrical components and biosensors, as well as in data processing of biomedical information. He authored *Synthesis and Optimization of Digital Circuits* (New York, NY, USA: McGraw-Hill, 1994) and has coauthored and/or coedited eight other books and more than 500 technical articles.

Dr. DeMicheli is a Fellow of ACM and a member of the Academia Europaea and the Scientific Advisory Board of IMEC and STMicroelectronics. He was the recipient of the 2012 IEEE/CAS Mac Van Valkenburg award for contributions to theory, practice and experimentation in design methods and tools and of the 2003 IEEE Emanuel Piore Award for contributions to computer-aided synthesis of digital systems. He received the Golden Jubilee Medal for outstanding contributions to the IEEE CAS Society in 2000, the D. Pederson Award for the best paper in the IEEE TRANSACTIONS ON COMPUTER-AIDED DESIGN OF INTEGRATED CIRCUITS AND SYSTEMS in 1987, and several Best Paper Awards, including DAC (1983 and 1993), DATE (2005) and Nanoarch (2010 and 2012). He has served IEEE in several capacities, including Division 1 Director (2008–2009), cofounder and President Elect of the IEEE Council on EDA (2005–2007), President of the IEEE CAS Society (2003), and Editor-in-Chief of the IEEE TRANSACTIONS ON COMPUTER-AIDED DESIGN OF INTEGRATED CIRCUITS AND SYSTEMS (1987–2001). He has been Chair of several conferences, including DATE (2010), pHealth (2006), VLSI SOC (2006), DAC (2000), and ICCD (1989).